JOURNAL OF MATERIALS SCIENCE 23 (1988) 4022–4026

Plasticity and space distribution of the phases in an iron/silver two-phase material

T. BRETHEAU, D. CALDEMAISON, A. FEYLESSOUFI, J. P. FONDÈRE, A. ZAOUI
L.P.M.T.M., C.N.R.S., Université Paris-Nord, Avenue J. B. Clément, 93430 Villetaneuse, France

In order to check the influence of the space phase distribution on the overall plastic behaviour of microinhomogeneous materials, a study of an iron/silver aggregate has been undertaken. The first results show a strong influence of phase concentration on the yielding and plastic flow stages. A qualitative explanation in terms of phase connectivity is proposed for yielding and a systematic discrepancy between a two-phase self-consistent model prediction and the experimental results is established for the plastic flow stage.

1. Introduction

To date, modelling of the plasticity of microinhomogeneous materials has been developed on the basis of explicit or implicit very strong hypotheses concerning the space distribution of the constituent phases. Thus, the uniform strain assumption of the Taylor model is equivalent (from a statistical point of view) to a parallel connection of the phases with respect to exterior loading, whereas the uniform stress assumption of the static model is equivalent to a series connection, and the self consistent scheme makes a peculiar hypothesis of disorder. None of the existing models can take into account an arbitrary spatial distribution of the phases; the only experimental information that is used is the phase volume fraction which can lead, at best, to upper and lower bounds for the overall plastic behaviour (by analogy with elasticity) [1], which is inadequate in the general case of two-phase materials [2].

In order to check the influence of the phase morphology on the overall plastic behaviour of materials, and to determine the mechanically relevant morphological parameters, a study of the deformation of a model two-phase material has been made, the first results of which are presented here.

2. Experimental details

2.1. Selection of a model two-phase material

For such a study, a suitable material must allow variation of the phase concentration in the full range without any modification of the phases themselves, and without drastic modification of the phase morphology; moreover, the plastic behaviour of the phases must be sufficiently different to be clearly distinguishable in the overall behaviour. The classical (technological) two-phase materials generally meet the second requirement, but the first is almost never fulfilled [3] because of evolution of phase composition and morphology with heat treatment, thus producing different phase concentrations. Thus a different route has been chosen for synthesizing a convenient two-phase material: the powder metallurgy technique. Powders of two insoluble metals, in the solid state, are mixed in any proportion and then sintered by hot isostatic pressing; the metallic binary elements that can be taken into account are FeAg, NiAg, CoAg which are insoluble, or FeCu, CoCu which are just slightly soluble [4]. Amoung these, FeAg has been chosen because of the very different plastic behaviour of the elements (see Section 3); in that manner both the above requirements are met. For the purpose of plastic deformation studies, this kind of material was previously prepared with a 50–50 concentration [5, 6].

2.2. Material production

Two powders are used for preparing the samples. (1) Iron powder (Poudmet 42 DR 100 R 150) in the as-received state has the chemical composition given in Table I and an apparent density between 2.6 and 2.8; it was screened to diameters between 65 and 100 μm. (2) Silver powder (Sogemet nagb 300) with a particle size lower than 50 μm, of 99.9% purity. The powders are mixed for 1 h in a planetary ball mill with 0.2% alcohol; then the mixture is poured into a metal tube (0.2 or 0.5 mm thick; 12 or 20 mm diameter, 100 or 200 mm long) and evacuate for 18 h under a secondary vacuum at room temperature prior to sealing. Hot isostatic pressing experiments are performed using argon as the pressure transmitting medium according to the temperature–pressure diagram of Fig. 1.

Tension test specimens with an 8 × 2 mm^2 cross-section and a 40 mm gauge length are machined from as compacted ingots then heat treated under pressure

TABLE I Chemical analysis of iron powder

	H_2	S	P	Mn	Si	C
Composition (wt %)	< 0.2	< 0.01	< 0.02	< 0.3	< 0.04	< 0.04

0022-2461/88 $03.00 + .12

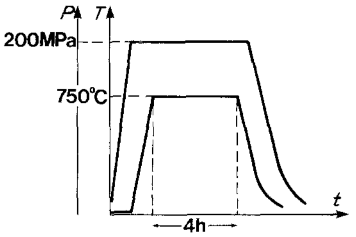

Figure 1 Schematic temperature and pressure against time diagram of the hot isostatic pressing experiments.

($T = 750°C$, $P = 200\,MPa$, $t = 5\,h$). The specimens are mechanically polished and some of them are submitted to a chemical etching (4% nital for iron and a saturated solution of $Cr_2O_3 + 10\%\ HCl$ for silver) to reveal the microstructure of each phase (Figs 2a and e).

Tension tests are carried out at room temperature in an Instron machine at a cross-head speed of 3×10^{-3} mm sec^{-1} ($\dot{\varepsilon} = 7.5 \times 10^{-5}\,sec^{-1}$).

2.3. Material characterization

Porosity in pure iron and silver is too low to be detected by the classical methods; in the two-phase materials, porosity seems to be of the same order, but confusion between a discrepancy in phase composition and the existence of a low porosity, may impede any measurement.

Typical microstructure of the two-phase Fe/Ag composite with varying concentration are shown in Fig. 2. One can observe a nearly continuous network of silver surrounding equiaxed iron grains even for fairly low silver concentrations; this is due to the smaller size and better ductility of silver powders that flow between the iron particles. It should be noted that neither a morphological nor a crystallographic texture can be detected.

A straightforward technique, based on X-ray microprobe analysis, allows the phase concentration to be determined and the macrohomogeneity to be checked; some samples with anomalous phase segregations (> 2% with a $5 \times 5\,mm^2$ analysed area) were

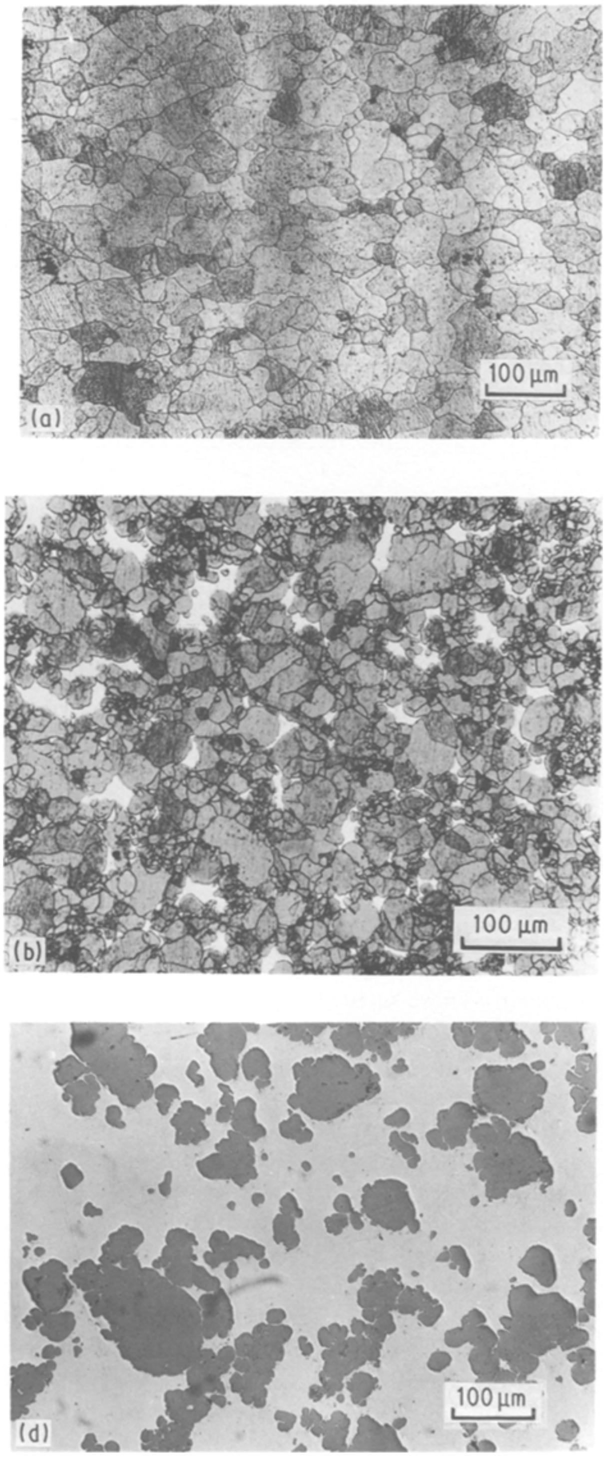

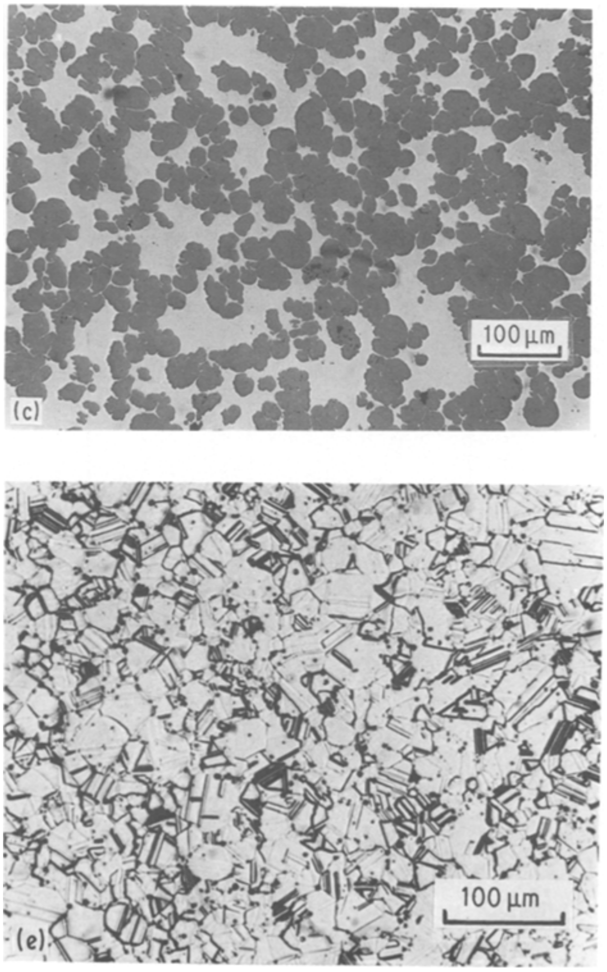

Figure 2 Optical micrographs of the microstructure for different concentrations: (a) iron phase (chemically etched); (b) 88% iron (iron is etched); (c) 50% iron; (d) 25% iron; (e) silver phase (chemically etched).

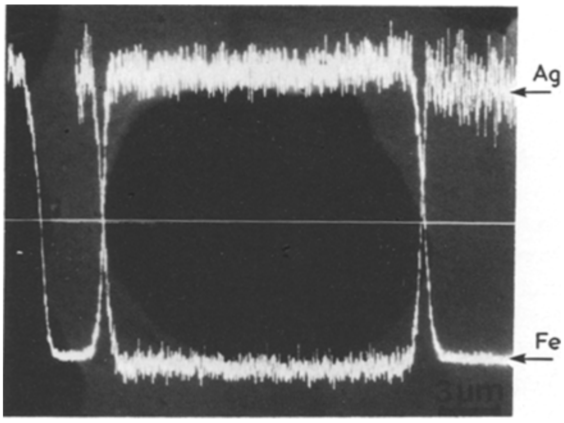

Figure 3 X-ray microprobe analysis along a line crossing phase boundaries. (Silver is grey and iron black.)

eliminated. No interdiffusion at the interphase boundary can be detected by X-ray microanalysis (Fig. 3); taking into account the microprobe characteristics, this means an interdiffusion zone thinner than a few micrometres.

Electrical resistivity measurements were made with a four-point probe, using conventional d.c. potentiometric techniques. A plot of resistivity against silver concentration is shown on Fig. 4. In the same figure, Hashin–Shtrikman bounds [7] are reported [1]. The good correlation between experimental points and the Hashin–Shtrikman lower bound is consistent with the structure of a material with iron included in silver in the main part of the concentration range. For the low silver concentrations, the two theoretical bounds converge and the experimental error does not allow the measurements to be correlated with a silver-included-in-iron model (ϱ_U) or an iron-included-in-silver model (ϱ_L).

$$\varrho_U = \varrho_1 \frac{3\varrho_2 + C_1(\varrho_1 - \varrho_2)}{3\varrho_2 + (\varrho_1 - \varrho_2)(C_1 + 3C_2)}$$

$$\varrho_L = \varrho_2 \frac{3\varrho_1 + C_2(\varrho_2 - \varrho_1)}{3\varrho_1 + (\varrho_2 - \varrho_1)(C_2 + 3C_1)} \qquad (1)$$

with ϱ_U and ϱ_L being the resistivity upper bound and lower bound, respectively, subscript 1 refers to iron and subscript 2 to silver. C_α is α-phase concentration.

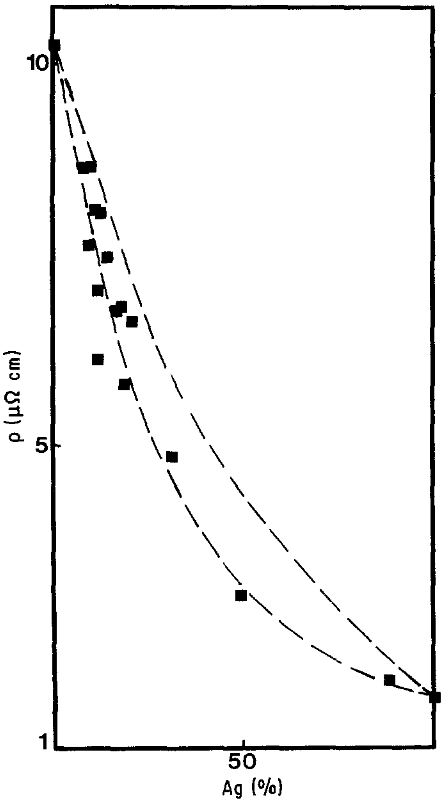

Figure 4 Conductivity plotted against silver concentration (T = 26° C). (■) Experimental points; (– – –) Hashin–Shtrikman bounds.

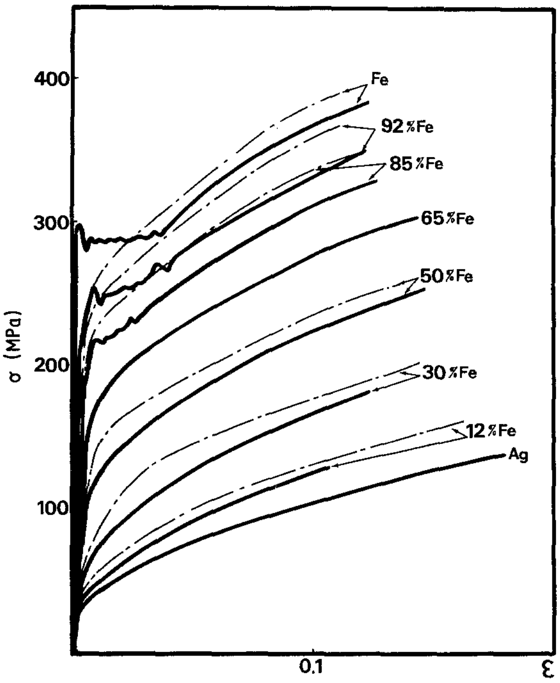

Figure 5 Stress–strain curves for the whole concentration range: (——) experimental, (– – –) theoretical curves.

3. Results and discussion

In this paper we shall mainly deal with the yielding behaviour of these materials; a forthcoming paper will be devoted to the analysis of the plastic flow.

3.1. Yielding behaviour

When a polycrystalline iron specimen (with some peculiar requirements: grain size not too big < 200 μm, iron containing small amounts of carbon or nitrogen) is stressed in tension, for a limiting stress one or more regions of local yielding are nucleated within the specimen. These yielded regions rapidly encompass the cross-section of the specimen and the stress drops (pure iron curve in Fig. 5) from the upper yield point (nucleating stress) to a value which allows the growth of these yielded bands (commonly referred to as Lüders bands) in the tensile direction along the gauge length of the specimen. The specimen continues to elongate at constant stress until the Lüders fronts have travelled the entire gauge length of the specimen. Generally, simple Lüders fronts are planar, and occur at an angle with the tensile axis which is still a debated question. The deformation of the specimen at larger strains occurs homogeneously with the rise in stress which is characteristic of strain hardening [8].

On the other hand, the yielding of a polycrystalline silver specimen occurs homogeneously without any

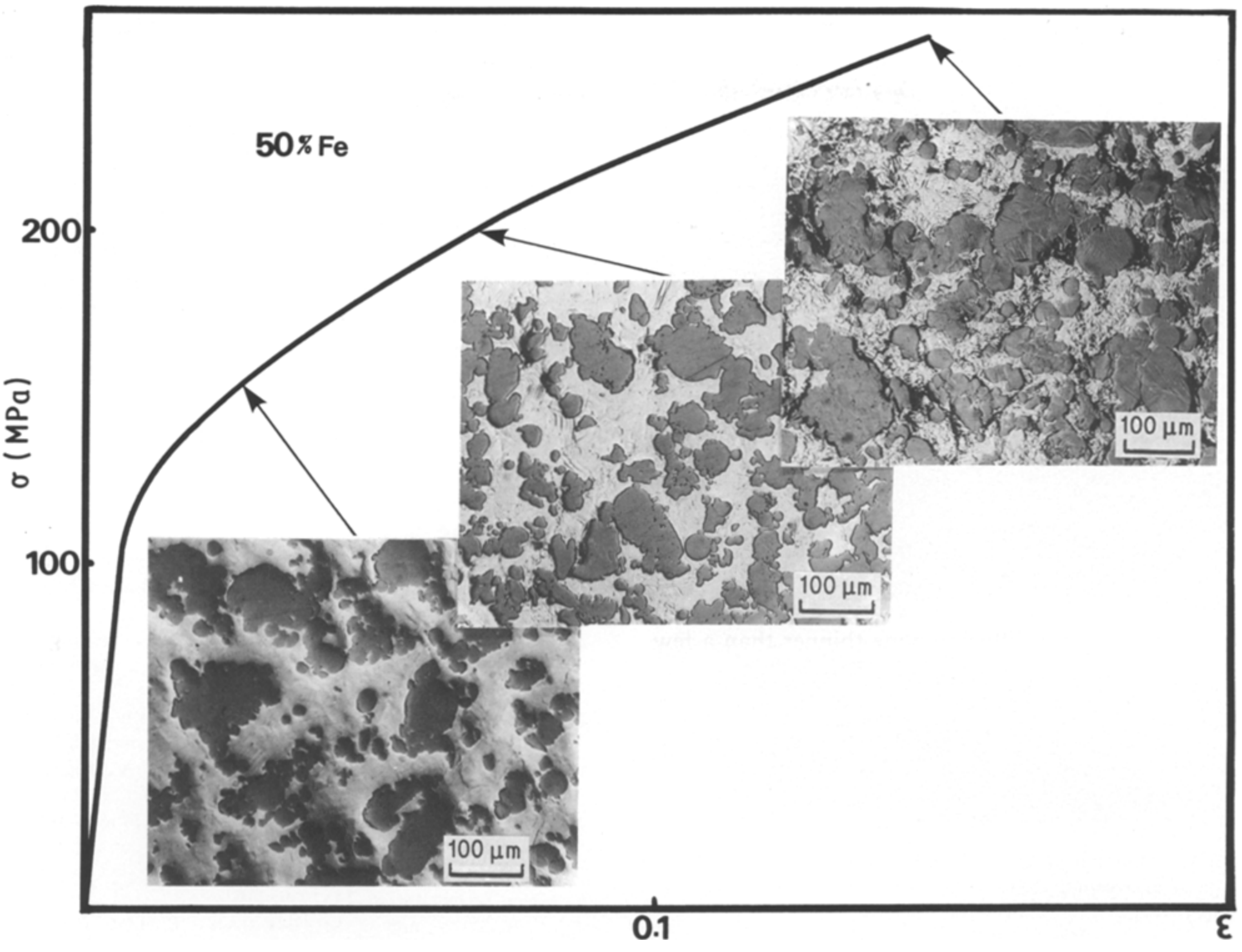

Figure 6 Stress–strain curve for 50% phase. As shown in the optical micrographs, silver yields first; then for about 10% strain, iron yields homogeneously without any front propagation.

front propagation, and the transition between elastic and plastic regimes gives rise to a smooth stress strain curve [8] (pure silver curve in Fig. 5).

In the case of two-phase materials, different types of behaviour are observed; they can be associated with different concentration ranges (Fig. 5): (a) from 100% to 85% Fe: silver and iron yield together by Lüders band propagation; (b) from 85% to 70% Fe: silver yields homogeneously first, then the deformation proceeds by band propagation; (c) less than 70% Fe: homogeneous yielding without band propagation; the lower the iron concentration, the later the occurrence of yielding in iron, but slip traces can be observed in iron at any concentration (Fig. 6).

In the case of inhomogeneous yielding, it can be noted that the plateau corresponding to the band propagation is shorter when the iron concentration is lower, and that it is no longer horizontal denoting a certain difficulty in the propagation. Moreover, a microscopical observation shows that the front propagates by a multiple nucleation of microbands ahead of the principal front (Fig. 7). Thus, a strong influence of the phase concentration on the yielding conditions can be observed. That kind of behaviour has been briefly reported on ferrite–martensite dual-phase steel [9], the Lüders strain decreasing with increasing martensite volume, and the Lüders bands vanishing for 40% martensite; porous iron behaves likewise, but with Lüders bands vanishing for a much lower porosity fraction (a few per cent) [10]. Of course, the Lüders band nucleation and propagation mechanism is not completely understood and the link between the grain behaviour and the aggregate inhomogeneous yielding is still missing, but the existence of a stress concentration at the front seems to be established [11]. Hence the front existence and propagation should depend on the possibility for a stress concentration to be transmitted by iron phase. An interpretation in terms of the percolation approach, as suggested by a recent work on elastic properties of two-phase materials [12], is inviting, but this theory does not seem to be yet sufficiently elaborated to be injected in real material plastic modelling. More simply we can say that a three-dimensional connectivity requirement for the iron phase, allowing the transmission of stress concentrations, is strongly suggested; of course the topological definition of that three-dimensional connectivity is not clear at present. Nevertheless, these experimental results mainly represent a stimulus to a better quantification of the material morphology in order to pin-point pertinent parameters showing a strong correlation with mechanical properties (A guide-line for the choice of tentative parameters can be found in a recent review by Hornbogen [13].)

3.2. Plastic flow behaviour

Here we are concerned with a homogeneous plastic flow regime appearing either just after the yield point

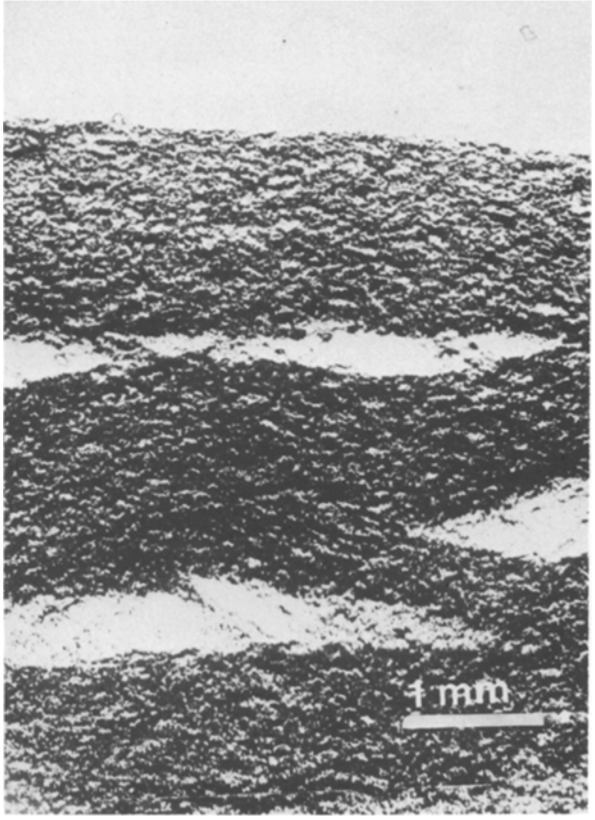

Figure 7 Optical micrograph of a Lüders band with multiple nucleation of microbands ahead of the principle front. (Vertical tensile axis.)

for lower iron concentrations ($< 70\%$), or after the Lüders band propagation stage for higher iron concentrations. A complete set of stress–strain curves has been obtained for the whole concentration range (Fig. 5). The comparison between the experimental results and some theoretical predictions is not straightforward. In fact, any law of mixtures using the pure iron stress–strain curve could forecast a plateau even for traces of iron in silver; but, within a wide concentration range, iron plasticizes without Lüders band propagation. Consequently, the prediction of the plastic flow behaviour at any concentration supposes the knowledge of an iron stress–strain curve without any plateau. In order to solve the difficulty, a "theoretical" pure iron curve was reconstructed using a two-phase self-consistent scheme [14] and taking into account the pure silver curve and the 65% iron curve (Fig. 5). After the Lüders plateau, the "theoretical" curve is very close to the experimental one. On the other hand, the experimental curves for lower iron concentrations fall systematically below the calculated curves, thanks to the self-consistent scheme. This is probably due to the application of an hypothesis of disorder to model the behaviour of an aggregate with a particular (even if it is not completely described) order.

A study is now in progress to elaborate a model which is able to deal with the peculiar arrangement of the phases and giving a better prediction of the real behaviour.

References

1. A. ZAOUI, in "Modelling small deformations of polycrystals", edited by J. Gittus and J. Zarka (Elsevier Applied Science, London, 1986) p. 187.
2. J. GURLAND, in "Yield, flow and fracture of polycrystals", edited by T. N. Baker (Applied Science, London, 1983) p. 51.
3. F. B. PICKERING, in Proceeding of the 4th Risø International Symposium on Metallurgy and Material Science, edited by J. B. Bilde-Sørensen, N. Hansen, A. Horsewell, T. Leffers, H. Liholt (1983) p. 183.
4. M. TAKAO and H. SENNO, *J. Magn. Magn. Mater.* **31–34** (1983) 949.
5. R. LE HAZIF, *Acta Metall.* **26** (1978) 247.
6. *Idem, Scripta Metall.* **13** (1979) 1103.
7. Z. HASHIN and S. SHTRIKMAN, *J. Appl. Phys.* **33** (1962) 3125.
8. B. JAOUL, in "Etude de la plasticité et application aux métaux" (Dunod, Paris, 1965) Ch. 8 and 9.
9. P. H. CHANG and A. G. PREBAN, *Acta Metall.* **33** (1985) 897.
10. J. W. HANCOCK, in "Yield, flow and fracture of polycrystals", edited by T. N. Backer (Applied Science, London, 1983) p. 69.
11. R. IRICIBAR, G. PANIZZA and J. MASSA, *Acta Metall.* **25** (1977) 1167.
12. R. A. TURUSOV, M. I. GAI, L. I. MANEVICH, V. G. OSHMIAN, E. S. ZEIENSKII, E. P. SULYAEVA, V. I. SOCHNEV, *Dokl. Akad. Nauk. SSSR* **211** (1986) 850.
13. E. HORNBOGEN, *J. Mater. Sci.* **21** (1986) 3737.
14. M. BERVEILLER and A. ZAOUI, *Res. Mech. Lett.* **1** (1981) 119.

Received 20 August 1987
and accepted 18 March 1988